

Intermediate Polars in a New (Optical) Light: Unprecedented Signal Detected in V709 Cas

L. Peters

Department of Physics, Durham University, Lower Mountjoy, South Rd, Durham DH1 3LE

(Submitted: August 11, 2022)

Flux detected in the optical can be analysed to give us the orbital, spin and beat periods for a magnetic cataclysmic variable. In this report, we fit Gaussian models to the frequency envelopes of Lomb-Scargle power spectra from TESS sectors 17, 18 and 19 in the intermediate polar V709 Cas, allowing the determination of the aforementioned periods. A new signal visible in its optical light curve is also detected due to the increased time-resolution and flux precision. We find periods of 5.3330 ± 0.0014 hr, 5.29878 ± 0.00003 min and 5.21247 ± 0.00003 min for the orbital, beat and spin signals, respectively. We postulate the new period, $P_\nu = 8.59802 \pm 0.00006$ min, to be the first ever detection of the p-mode oscillations from the secondary star, though await further investigations in the field of asteroseismology to confirm this.

I. INTRODUCTION

On the 18th April 2018, the Transiting Exoplanet Survey Satellite (TESS) was launched to discover thousands of planets orbiting our nearest, brightest stars [1]. In particular, these stars are exoplanets, which have been detected via the transit method. On its primary mission, the survey was executed by tiling the sky into 26 sectors with a $24^\circ \times 96^\circ$ field of view. Every sector was observed for 27.4 days, and the apparent brightness of the detected objects was recorded with a resolution of two minutes. During these two years, 2241 exoplanet candidates were detected [2] and by the end of 2021, more than 5000 candidates had been detected [3], providing a plethora of objects to be rigorously researched in succeeding years.

In addition to the primary mission, TESS has enabled the general scientific public to request specific targets for ex-traneous research. Consequentially, the time-flux measurements for thousands of Cataclysmic Variables (CVs) has been made accessible, and with this unparalleled precision for such an enormity of targets, researchers have the potential to explore these objects with a clarity in the optical range never before accessible.

CVs comprise a white dwarf (WD) in a close binary system with a secondary star. Due to this close proximity between the WD and its secondary, mass transfers from the donor star onto the WD via Roche-lobe overflow. Within CVs, some systems contain a magnetic WD with a field of ≥ 1 MG; the subset containing the weakest range of fields (≈ 1 -10 MG) [4] are known as intermediate polars (IPs). In addition to this weak field, they feature a cool, main-sequence red dwarf secondary. IPs rotate super-synchronously ($P_{orb} > P_{spin}$) [5] with typical orbital periods of 3-7 h [6]. In these systems, a stream of stellar material leaves the donor star at the inner Lagrangian point, L_1 , and due to the perpendicular orbital motion at L_1 , the stream carries an angular momentum that swings it into orbit around the WD. This orbiting material forms an accretion disk up to the point at which magnetic pressure surpasses the ram pressure output by the accreting gas. At this point, the disk is truncated and the material flows along the WD's field lines to its magnetic poles. As the material reaches these poles, the accretion columns impact the WD surface and cause a shock within themselves, which releases hard X-rays via thermal bremsstrahlung [7], [8]. For IPs, due to the detection of P_{orb} , P_{spin} and the beat from $P_{spin} - P_{orb}$, P_{beat} , the mechanism governing the accretion is disk-overflow [9].

Using TESS to evaluate the aforesaid periods of several IPs, we revisit a target thought to have been studied to a

comprehensive extent: V709 Cas. However, in light of the new data made available by TESS, V709 Cas is displaying a new signal never before reported. This journal summarises our current knowledge on the target, and provides updated values for the orbital, spin and beat periods. It also makes speculations on the cause of the recently-detected signal, which has never been observed in any CV.

II. OBTAINING THE SIGNALS

Specific to V709 Cas, TESS recorded data in sectors 17, 18 and 24, which span respectively from the 7th of October to 2nd of November, 2019; the 3rd of November to the 27th of November, 2019; and to the 16th April to 12th May, 2020.

From these data observed by TESS, the flux and time were plotted to produce a light curve in all three sectors, as illustrated in figure 1.

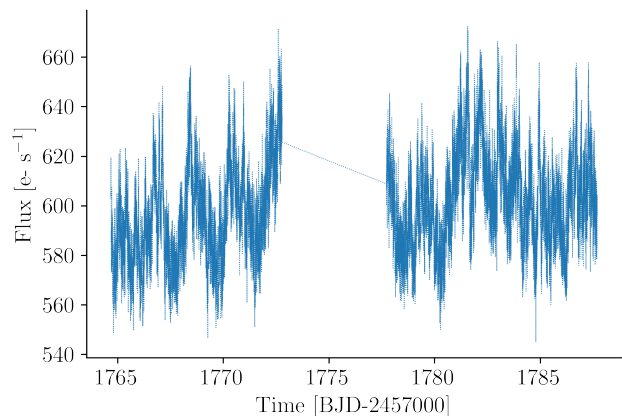


FIG. 1: Optical light curves obtained from TESS sector 17. Notice the sinuous pattern, suggesting there are periodical signals present in the power spectra V709 Cas as expected in a CV. The gap from 1772.8 to 1777.7 BJD - 2457000 is the offloading period during which the collected data are transmitted back to Earth so that the satellite can clear its RAM and continue to record.

Transforming this light curve into a power spectrum through python employs `astropy.timeseries.LombScargle()`; this class enables the user to compute a Lomb-Scargle periodogram [10], [11] and thus detect periodic signals from irregular observations. Within `LombScargle`, the `.autopower()` method was implemented to compute the power at automatically determined frequencies, where frequency, f , $0 \leq f \leq f_n$ and f_n is the Nyquist frequency for a sampling rate of 2 min: 360 cycles per day.

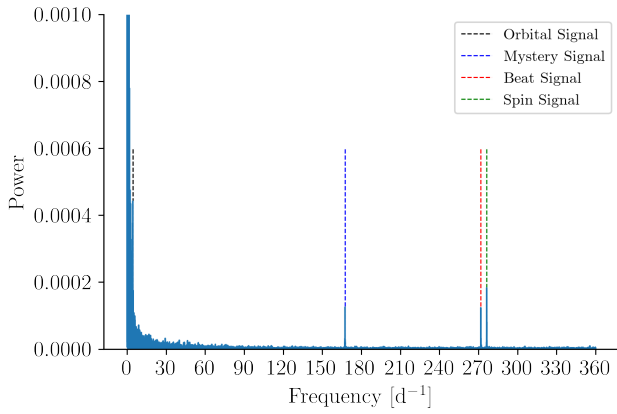


FIG. 2: Power spectrum obtained from compiling TESS sectors 17, 18 and 24. Four signals are visible in black, blue, red and green - corresponding to the orbital, mystery, beat and spin frequencies respectively. The y-axis has been maximised so that all frequencies are detectable - the scaling is not important to this journal, as mentioned in the discussion.

Figure 2 displays four detectable signals in V709 Cas. Present are the orbital, spin and beat ($f_{spin} - f_{orb}$) signals, as well as the 'mystery' signal at $\approx 167 \text{ d}^{-1}$. In order to precisely calculate their periods, it was necessary to 'zoom-in' on the periodogram and analyse each frequency individually. The frequency range was limited to contain only the peak corresponding to a given frequency, and a Gaussian function was fitted against this through `scipy.optimize.curvefit()` in python. The centroid of the Gaussian model then provided our frequency for a given signal at its max intensity and the standard deviation provided an estimate error. These frequencies were then also converted into periods.

III. RESULTS

Having fitted the Gaussian as outlined above, table 1 details the periods and frequencies for all four signals detected in the light curve of V709 Cas from TESS sectors 17, 18 and 19, and from all three sectors compiled into one array. Figure 3 shows the neighbourhood of frequencies surrounding the mystery signal at maximum intensity, as well as a zoomed in subplot to accentuate the Gaussian model plotted over the peak, and the corresponding centroid.

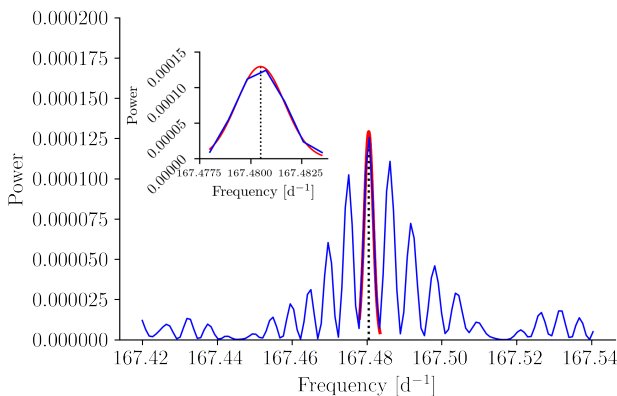


FIG. 3: V709 Cas power spectrum obtained from compiling TESS sectors 17, 18 and 24 (blue) with the Gaussian function modelled over the maximum peak (red). This figure focuses on the region surrounding the new 'mystery' frequency.

For the compiled data, f_{ν} , the determined frequency for the mystery signal, was $167.4805 \pm 0.0012 \text{ d}^{-1}$. This corresponds to a period of $8.59802 \pm 0.00006 \text{ min}$.

Similar graphs were plotted for the orbital, spin, and their related beat frequencies in figure 4.

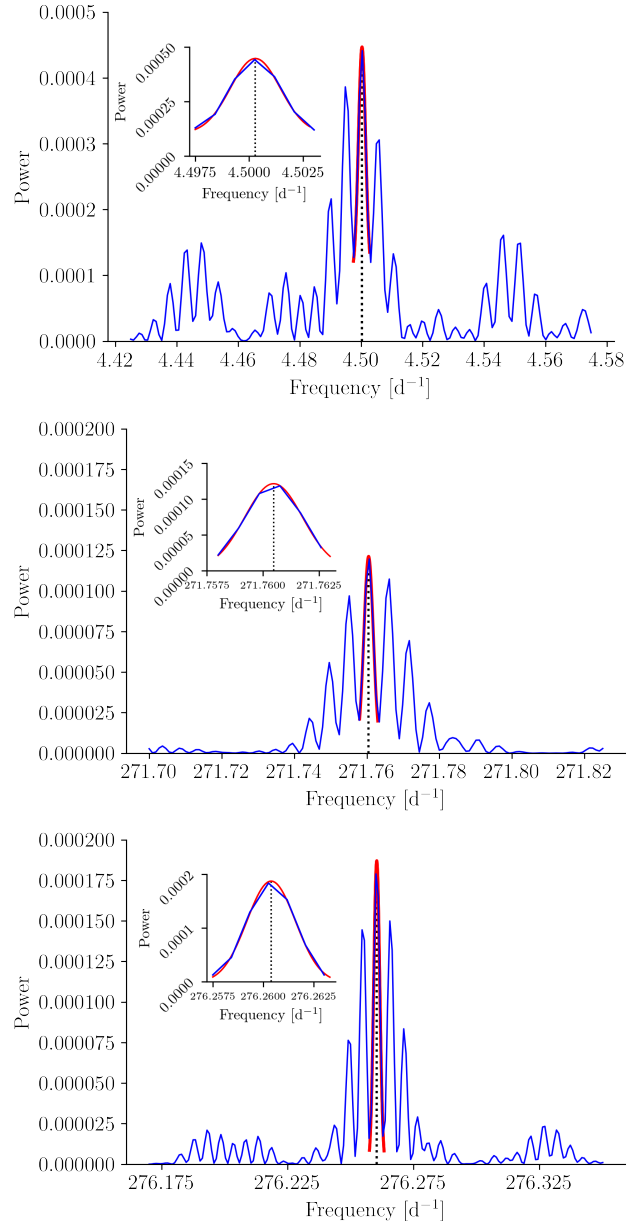


FIG. 4: V709 Cas power spectra obtained from compiling TESS sectors 17, 18 and 24 (blue) with the Gaussian function modelled over the maximum peak (red). The top, middle and bottom plots focus on the regions surrounding the orbital, beat and spin frequencies respectively.

The frequencies and corresponding periods deduced from figure 4 are $4.5003 \pm 0.0011 \text{ d}^{-1}$ and $5.3330 \pm 0.0014 \text{ hr}$ for f_{orb} , P_{orb} ; $271.7605 \pm 0.0012 \text{ d}^{-1}$ and $5.29878 \pm 0.00003 \text{ min}$ for f_{beat} , P_{beat} ; and $276.2604 \pm 0.0012 \text{ d}^{-1}$ and $5.21247 \pm 0.00003 \text{ min}$ for f_{spin} , P_{spin} .

IV. DISCUSSION

Periods calculated in this report are consistent with previously published literature (see i.), providing reason to believe that the new period is a legitimate detection of a mechanism never before observed in a CV. As the orbital, beat

Signal	Compiled		Sector 17		Sector 18		Sector 24	
	f [d ⁻¹]	Period*	f [d ⁻¹]	Period*	f [d ⁻¹]	Period*	f [d ⁻¹]	Period*
Orbital <i>P(hr)</i>	4.5003 ± 0.0011	5.3330 ± 0.0014	4.51 ± 0.02	5.33 ± 0.03	4.49 ± 0.02	5.34 ± 0.03	4.49 ± 0.02	5.34 ± 0.03
Mystery <i>P(min)</i>	167.4805 ± 0.0012	8.59802 ± 0.00006	167.470 ± 0.014	8.5985 ± 0.0007	167.492 ± 0.015	8.5974 ± 0.0008	167.478 ± 0.014	8.5981 ± 0.0007
Beat <i>P(min)</i>	271.7605 ± 0.0012	5.29878 ± 0.00003	271.757 ± 0.016	5.2989 ± 0.0003	271.766 ± 0.016	5.2987 ± 0.0003	271.764 ± 0.014	5.2987 ± 0.0003
Spin <i>P(min)</i>	276.2604 ± 0.0012	5.21247 ± 0.00003	276.262 ± 0.014	5.2124 ± 0.0003	276.259 ± 0.015	5.2125 ± 0.0003	276.264 ± 0.0153	5.2124 ± 0.0003

TABLE I: Results for all four of the signals detected in the optical for each TESS Sector, and the signal presented when all three sectors are compiled.

* All reported orbital periods are given in hours, and all remaining periods are given in minutes.

and spin periods are still detected in simultaneity with this new period, we can rule out trivially (see ii.) that the physics governing this system has not changed.

Analytically, the error for the frequencies determined in this report was taken to be the standard deviation of our plotted Gaussian. In order to be more precise, it is necessary to perform a Monte Carlo simulation. This was omitted from this report due to lack of time. Furthermore, in figure 4, the Gaussian sub-plots for the orbital and beat signal appear to plateau at a non-zero value. This is simply due to the fact that as the power is $\ll 1$ and the plot covers such a small range of values, the model appears to level at ≈ 0.00001 . This difference is negligible. The powers calculated via the `.autopower()` method may seem to undermine the validity of these signals since they appear to have low intensity. However, this is a consequence of the noise at the beginning of the spectrum being significantly larger than the noise after 60 d⁻¹ (figure 2). When one compares the signal to the noise level in the vicinity of a given frequency, the relative strength of the signals is demonstrated.

As far as previous literature is concerned, whether centred around V709 Cas or focused on different objects, a fourth signal in this time range has never been detected - a new variability was thought to be detected in V709 Cas with a period of 23.7 minutes [12]. However, the validity of the results is discussed in the subsequent section, as we comprehensively summarise the current knowledge of this target.

i. History of V709 Cas.

In 1995, V709 Cas was discovered during the ROSAT survey [13] due to its consistency with intrinsically absorbed thermal bremsstrahlung from IPs known before ROSAT. The ROSAT survey then revealed that V709 Cas exhibits a double-peak X-ray pulse profile [14]. Norton postulated that since the profile's two maxima were relatively closely spaced, the location of the lower and upper magnetic poles may be asymmetrical. This asymmetry was thought to be caused by a dipole magnetic field offset from the centre of the WD. Norton et al. detected a P_{spin} of 312.78 ± 0.03 s, which, within error, is consistent with all individual sectors of TESS data; however, they did not detect any orbital, beat, sideband or harmonic signals. From this, they concluded that the inclination angle of this system is low, and

that it must be a disk-fed accretor. From the aforementioned short spin period, they deduced that the target has a weak magnetic field. Accordingly, the radius at which material is captured by the field lines is relatively small, which in turn reflects a notable footprint of accretion curtains. V. P. Kozhevnikov observed V709 Cas between 4th - 9th October 1999 using a three-channel photometer and 70 cm telescope at Kourouka Observatory. In his observations, he identified a $P_{spin} = 312.77 \pm 0.04$ s, and also a $P_{beat} = 317.94 \pm 0.04$ s, both in agreement with the values reported in this journal, as well as a weak periodic signal corresponding to the first harmonic of P_{spin} [15].

In a study of emission line radial velocities [16], Bonnet-Bidaud et al. managed the signal aliases in order to determine $P_{orb} = 0.2225 \pm 0.0002$ days, or 5.34 ± 0.012 hours, which aligns with the orbital period from all TESS data, within error. They report broad absorption (equivalent width of $\approx 2-4$ Å) which influences the Balmer lines from $H_\delta - H_\beta$. They attribute the broad absorption to the atmosphere of a DA (only hydrogen features) $\log(g) = 8$ (in cgs units, $\approx 0.6 M_\odot$) WD at a temperature $\approx 23,000$ K - which is on the upper-limit of temperatures recorded for magnetic CVs [17]. Bonnet-Bidaud et al. concluded that dwarf-nova events are precluded due to the steadiness of the optical flux and that the absence of He absorption does not satisfy a disk origin star. Furthermore, the lack of outstanding absorption around H_α implies that the spectral component responsible for absorption has a steep continuum, mainly contributing to the blue, and becoming minor in the red due to dilution through the rest of the emission. This led Bonnet-Bidaud to conclude that this was the first direct detection of a WD in an IP system. In their paper, they query why V709 Cas was the only (at the time) IP where the WD is seen to contribute significantly to the overall flux so that the atmospheric absorption becomes visible, and that there is no indication the white dwarf is atypical. However, in light of the new signal detected in this report, it could be argued that the system is unique or amplified, and this is why V709 Cas presents the first direct detection of a WD, and the first direct detection of this new signal in any CV.

Considering the RXTE and BeppoSAX observations of V709 Cas, further X-ray observations reinforce that V709 Cas is a disk accretor due to the presence of $P_{spin} = 312.75$

s, but no X-ray orbital or sideband period [18]. In addition to the spin, De Martino recorded that the amplitude of the spin pulsation increased, but the X-ray flux decreased. This variation over time signifies that the system's mass accretion fluctuates on the timescale of less-than months, to years. These observations also revealed V709 Cas' spectrum to be hard and compatible with an optically thin, isothermal plasma at 27 keV, featuring complex absorption and an iron K_α fluorescent line due to reflection from the WD surface. In the pre-shock region, cool and ionised absorbing material is exhibited. They attribute the low-energy range complex absorption to the rotational period, and the high-energy pulsation to the presence of a non-zero shock height above the accretion poles.

The INTEGRAL telescope then enabled the hard X-ray time-averaged spectrum of V709 Cas to be produced [19]. Using different multi-temperature and density X-ray post-shock models, the study by Falanga et al. reevaluated the post-shock temperature to be ≈ 40 keV. This post-shock temperature concurs with their Bremsstrahlung temperature of ≈ 26 keV - refining the values given by De Martino (2001). $T_{Brem} < T_{shock}$ since T_{Brem} constitutes a weighted mean value between the T distribution from V709 Cas' surface to the shock height. In comparison to the $\approx 0.6 M_\odot$ WD mass reported in Bonnet-Bidaud et al's above paper, Falanga et al. employed the JEM-X X-ray monitor between 5-20 keV and relevant ISGRI data from 20-100 keV to estimate the target's mass to be $0.82^{+0.12}_{-0.25} M_\odot$. Furthermore, from the mass-radius relation for WDs [20], they determined the radius of the WD in V709 Cas, $R_{WD} = (0.68 \pm 0.13) \times 10^9$ cm.

In 2008, RXTE and INTEGRAL observations led to a new time-averaged, broad-band X-ray spectrum of V709 Cas, for which the post-shock region was reconfigured to include Compton scattering [21] so that its influence on the structure of the post-shock region and subsequent spectrum could be considered. Suleimanov revealed that Compton scattering only becomes significant at high accretion rates and high WD masses. They calculated $R_{WD} = 0.61 \times 10^9$ cm, which provided a mass-accretion rate of $\dot{M} = 0.8 \times 10^{16}$ g s $^{-1}$. Therefore, for a low accretion rate star such as V709 Cas [22] for a list of accretion rates for WDs), there was little difference between M_{WD} modelled with Compton scattering and without: $M_{WD} = 0.91 \pm 0.02 M_\odot$ and $0.88 \pm 0.02 M_\odot$, respectively. Both masses are consistent with the reported value in Falanga 2005, but the error for M_\odot in Falanga et al. is noticeably large.

The white-light flickering present in V709 Cas was identified in-line with the $\alpha - \Sigma$ diagram from the Fritz and Bruch classification scheme [23]. For the energy distribution of flickering at different timescales, α , and the strength of flickering on a given timescale, Σ , V709 Cas populates the same region as magnetic systems [24]. Its values cover intervals $0.9 < \alpha < 1.8$ and $-1.3 < \Sigma < -0.6$, which are consistent with magnetic CVs [25]. In the report, Tamburini et al. also state that α and Σ seem anti-correlated, and that the flickering is self-similar with stochastic persistent memory through a timescale ranging from tens of minutes to 10 s. The study claims that since they are able to detect P_{spin} in the X-ray, but not optical, their method can be used to characterise CV subtypes. The validity of this claim is now questioned since in later research, such as this paper, P_{spin} has been detected in the optical.

The Suzaku satellite led to the estimate of masses for sev-

eral nearby IPs. V709 Cas was among those IPs, and a WD mass equal to $1.22^{+0.05}_{-0.20} M_\odot$ was calculated [26]. This is far greater than any of the previously-mentioned M_{WD} , the implications of which are discussed in [27]. As well as the mass estimate, the Suzaka satellite observed V709 Cas to have a RA = 7.204 and declination = 59.289. In 2010, V709 Cas was studied through the acquisition of time-series radial-velocity spectroscopy and P_{orb} was determined to be 5.33288 hours [28]. P_{orb} is considered more precise here due to the longer time base. Thorstensen et al. could not confirm the WD detection claimed by Bonnet-Bidaud et al. due to the lack of absorption wings around H_β in any of the observed runs and non-detection of the secondary. Thorstensen et al. question the lack of evidence for the presence of the secondary, if the system's luminosity is low enough for a relatively faint WD to be seen. This report may answer their query from a decade ago, as we consider its implication in section ii.

As mentioned in the introduction to this section, a new signal was detected at 23.7 minutes in photometric CCD observations from the VNT (Hric, 2014). It is proposed that the period could be due to vibration of the accretion stream in the magnetic field of the WD. Hric et al. further imply that these vibrations could relate to dynamical instabilities in the accretion curtains. Hric et al. claim this new period is visible in Norton, 1999, Fig. 5 and Kozhevnikov, 2001, Fig. 3. Specifically, this 23.7 min signal corresponds to 60.79 d $^{-1}$, or 0.704 mHz, for which there is no evidence of a signal distinguishable from noise in the aforementioned figures. Furthermore, the signal is also not visible in TESS and we therefore argue that this detection can be ruled out as a new signal due to the high precision of TESS. Regarding the better-known signals, they calculated $P_{orb} = 0.2222123$ d via (O-C) analysis, with an error estimate of the same magnitude as reported in Thorstensen et al. (2010); P_{spin} was calculated on individual nights, and on their 'best night' they report $P_{spin} = 311.8$ s.

Due to the NuSTAR and XMMNewton missions, increased observation sensitivity provided new insight into the shock height and spin modulation for V709 Cas - and also led to the first detection of its Compton hump [29]. Mukai et al validate the >10 keV modulation evident in de Martino (2001) and posit this is due to the X-ray releasing region above the WD. The observed low reflection amplitude and relatively weak 6.4 keV line in Mukai et al's study is also in conjunction with de Martino (2001). For the WD shock height $\approx 0.2 R_{WD}$ originally proposed by de Martino (2001), Mukai claims one would expect horizon and viewing angles and a reflection amplitude that coincide with their observations. Despite extensive agreement with de Martino et al. (2001), Mukai et al. were unable to verify the ionised Fe K edge at ≈ 8.0 keV.

Further analysis of the NuSTAR X-rays led to direct measurements of M_{WD} in V709 Cas [27]. By fitting an accretion column model to spectra in a range of 3-78 keV, the mass is estimated for different models. For the IP mass model with reflection, freezing the fraction of reflected-downward radiation to unity and allowing the inclination angle of the reflecting surface, θ , to vary, $M_{WD} = 0.88^{+0.05}_{-0.04} M_\odot$ with $\cos\theta = 0.62^{+0.24}_{-0.20}$. In a simple IP mass model, $M_{WD} = 0.91 \pm 0.05 M_\odot$. Considering the more accurate mass to be the one accounting for reflection, their mass measurement is consistent with Falanga (2005) and Suleimanov et al. (2008), though not Yuasa et al. (2010).

Shaw et al., however, recognise that Yuasa et al. do not account for reflection, and illustrate how this can lead to an unacceptable fit. Finally, Shaw et al. argue that the low spin period of V709 Cas suggests that the magnetosphere radius, R_m , may be close to the WD surface. Again using Nauenberg (1972), they calculate $R_m = 10.5R_{WD}$ for a $0.88M_{\odot}$ WD, which in accordance with Suleimanov et al. (2016) [30], is not in close enough proximity to the WD to have a non-negligible effect on the derived M_{WD} .

There has been no research published on V709 Cas involving analysis from the data obtained from TESS.

ii. Postulating the cause of the Mystery Signal.

Having summarised the current knowledge of this target, we are left with few ideas as to what could be causing this new period at 8.59802 minutes. In this section, various reasons are proposed as an attempt to reach a conclusion via exclusion for the mechanism governing this signal.

Immediately, we can negate it being the true spin period of V709 Cas since we are still able to detect the orbital sideband of the spin frequency, as well as the spin period, with values that agree with published literature. Similarly, it cannot be a harmonic beat period as for integers x and y , $xf_{spin} - yf_{orb} \neq f_{\nu}$. The closest value to f_{ν} using the results for the compiled data in table 1 is when $x = 1$, $y = 24$, $xf_{spin} - yf_{orb} = 168.2532$. We did not consider $x > 1$ as the probability of this beat harmonic is exceedingly low.

Ruling out the possibility of the signal corresponding to those previously detected, we consider the physical qualities of V709 Cas. The feasibility that this signal comes from the accretion disk is low, since f_{ν} would be broader due to the disk being so wide: each infinitesimal 'ring' of the disk is at a different radius, and by Kepler's 2^{nd} law, should move with varying velocity. Varying velocity would realise different periods, which would result in a flatter, broader signal detected. That we see a width of the same order of magnitude as the other signals confirms that this signal cannot come from the accretion disk.

Tamburini et al. (2009) report (as above) stochastic persistent memory flickering on a timescale ranging from tens of minutes to tens of seconds. This includes the new period detected in this report, however, we are unaware of the relevance of this signal in relation to flickering.

As first queried by Thorstensen et al. (2010), if the WD was able to be detected by Bonnet-Bidaud (2001), why have we not been able to notice the secondary in this system? It is most probable that this new period corresponds to such a signal. In solar-like stars, repeated signals of stochastic excitation and damping by turbulent motions in the external convective layers lead to a myriad of resonant modes [31]. Since we know V709 Cas is an IP, its donor star is a cool, main-sequence red dwarf, and hence, can be considered solar-like. Most observed in solar-like pulsators are p-modes: modes which are restored by pressure waves and are characterised by their large amplitudes in the envelope of the star, as well as their dominant radial motion [32].

P-mode envelopes are centered at $\approx 2160 \mu\text{Hz}$ in 16 Cyg A, another solar-like star, and $\approx 3000 \mu\text{Hz}$ in our sun [33]. The new signal in this report is in the range 1938.310 - 1938.565 μHz , and so it is certainly possible that we are detecting the frequency at maximum power for a p-mode envelope in the secondary star of V709 Cas. Garcia and Ballot's review (2019) also discusses the effects of rotation and magnetic fields on the oscillations of solar-like stars.

Perhaps the asymmetries produced through this variability could explain the difference between the variations between TESS sectors. In CVs, most secondary stars are tidally locked which would provide reason for the detection of only one signal, and not another associated with its spin.

With regard to why V709 Cas is potentially the only IP to allow the detection of the secondary star's p-mode oscillation in the optical, it is possible that, as mentioned in Thorstensen (2010), V709 Cas' luminosity is so low that flux from the secondary star is detectable. There is uncertainty as to what could cause this, and even that the hypothesised p-modes are in fact responsible for the new period. It is clear that more research is needed to clarify the nature of this new signal.

V. CONCLUSIONS

Through the analysis of TESS data, this journal provides an updated set of signals corresponding to the orbital, spin and beat periods. We also discuss a new 'mystery' signal at 8.59802 ± 0.00006 minutes, which we propose to be the first ever detection of the secondary star in an intermediate polar following a review of previous literature published on this target. Further to this report, more rigorous analysis via asteroseismological methods may be able to confirm our proposition, and the continual development in the quality of satellites will lead to an increased volume of detections similar to that featured in this report.

Acknowledgments

I am grateful to S. Scaringi for not only the great insight he provided throughout the conducting of this research, but also the patience and time he took to introduce me to Cataclysmic Variable stars to begin with.

Furthermore, I would like to thank all of those referenced in this journal. Their research was invaluable to help develop my understanding of this target for the duration of this project. This research utilised the MIT-led NASA mission, TESS. I am thankful to all those responsible for the successful enabling of this mission.

References

- [1] R. Garner, 'About TESS', NASA, Jul. 15, 2016. <http://www.nasa.gov/content/about-tess> (accessed Aug. 02, 2022).
- [2] N. M. Guerrero, 'The TESS Objects of Interest Catalog from the TESS Prime Mission', *The Astrophysical Journal Supplement Series*, p. 29 (2021).
- [3] N. Guerrero, 'TESS Science Office at MIT hits milestone of 5,000 exoplanet candidates'. <https://tess.mit.edu/news/tess-science-office-at-mit-hits-milestone-of-5000-exoplanet-candidates/> (accessed Aug. 02, 2022).
- [4] Hellier, C. *Cataclysmic Variable Stars - How and why they vary*, 1st ed. Chichester, Praxis Publishing, p. 135 (2001).
- [5] J. C. Lurie et al., *Tidal Synchronization and Differential Rotation of Kepler Eclipsing Binaries*, *AJ*, **154**, 6, p. 250 (2017), doi: 10.3847/1538-3881/aa974d.
- [6] V. Breus, I. L. Andronov, P. Dubovsky, K. Petrik, and S. Zola, *On the spin and orbital variability of the intermediate polars*, arXiv, (2019).
- [7] K. Aizu, *X-Ray Emission Region of a White Dwarf with Accretion*, *Prog. Theor. Phys.* **49**, 4, p. 11, (1973).

- [8] A. J. Norton et al., *On the interpretation of intermediate polar X-ray power spectra*, Mon. Not. R. Astron. Soc. **280**, 937–952 (1996).
- [9] Hellier, C., *Disc-Overflow Accretion in Intermediate Polars*, Adv. Space Res. **22**, 7, pp.973–980 (1998).
- [10] N. R. Lomb, *Least-squares frequency analysis of unequally spaced data*, Astrophys Space Sci. **39**, 2, pp. 447–462, (1976), doi: 10.1007/BF00648343.
- [11] J. D. Scargle, *Studies in Astronomical Time Series Analysis. II.*, ApJ. **263**, 835–853, (1982).
- [12] L. Hric et al., *The new period of the intermediate polar V709 Cas*, Astron. Nachr. **335**, 4, 362 – 366, (2014), doi: 10.1002/asna.201312044
- [13] F. Haberl and C. Motch, *New Intermediate Polar Discovered in the ROSAT survey: two spectrally distinct classes*, A&A. **297**, L37–40, (1995).
- [14] A. J. Norton, A. P. Beardmore, A. Allan, and C. Hellier, *YY Draconis and V709 Cassiopeiae: two intermediate polars with weak magnetic fields*. arXiv, (1998).
- [15] V. P. Kozhevnikov, *Detection of optical oscillations of the intermediate polar V709 Cassiopeae (RX J0028.8+5917)*, A&A. **366**, 3, pp. 891–897, (2001), doi: 10.1051/0004-6361:20000259.
- [16] J. M. Bonnet-Bidaud, M. Mouchet, D. de Martino, G. Matt, and C. Motch, *The white dwarf revealed in the intermediate polar V709 Cassiopeiae*, A&A. **374**, 3, pp. 1003–1008, (2001), doi: 10.1051/0004-6361:20010756.
- [17] E. M. Sion et al., *An IUE and HST Archival Study of the Hot White Dwarf in the Symbiotic Variable RW Hydrae*, AJ. **123**, 983–987 (2002).
- [18] D. de Martino et al., *The X-ray emission of the intermediate polar V 709 Cas*, A&A. **377**, 2, pp. 499–511, (2001), doi: 10.1051/0004-6361:20011059.
- [19] M. Falanga, J. M. Bonnet-Bidaud, and V. Suleimanov, ‘INTEGRAL broadband X-ray spectrum of the intermediate polar V709 Cassiopeiae’, A&A. **444**, 2, pp. 561–564, (2005), doi: 10.1051/0004-6361:20054002.
- [20] M. Nauenberg, *Analytic Approximations to the Mass-Radius Relation and Energy of Zero-Temperature Stars*, ApJ. **175**, 417, (1972), doi: 10.1086/151568.
- [21] V. Suleimanov, J. Poutanen, M. Falanga, and K. Werner, *Influence of Compton scattering on the broad-band X-ray spectra of intermediate polars*, A&A. **491**, 2, pp. 525–529, (2008), doi: 10.1051/0004-6361:200810119.
- [22] M. M. Shara, D. Prrialnik, Y. Hillman, and A. Kovetz, *The Masses and Accretion Rates of White Dwarfs in Classical and Recurrent Novae*, ApJ. **860**, 2, p. 110, (2018), doi: 10.3847/1538-4357/aabfbd.
- [23] T. Fritz, A. Bruch, *Studies of the Flickering in Cataclysmic Variables*, A&A. **332**, 586–604, (1998).
- [24] F. Tamburini, D. de Martino, and A. Bianchini, *Analysis of the white-light flickering of the intermediate polar V709 Cassiopeiae with wavelets and Hurst analysis*, A&A. **502**, 1, pp. 1–5, (2009), doi: 10.1051/0004-6361/200911656.
- [25] A. Bruch, *Flickering in Cataclysmic Variables: its properties and origins*, A&A. **266**, 237–265, (1992).
- [26] T. Yuasa et al., *White dwarf masses in intermediate polars observed with the Suzaku satellite*, A&A. **520**, p. A25, (2010), doi: 10.1051/0004-6361/201014542.
- [27] A. W. Shaw, C. O. Heinke, K. Mukai, G. R. Sivakoff, J. A. Tomsick, and V. Rana, *Measuring the masses of Intermediate Polars with NuSTAR: V709 Cas, NY Lup and V1223 Sgr*, MNRAS. **476**, 1, pp. 554–561, (2018), doi: 10.1093/mnras/sty246.
- [28] J. R. Thorstensen, C. S. Peters, and J. N. Skinner, *Optical Studies of 20 Longer-Period Cataclysmic Binaries*, PASP. **122**, 897, pp. 1285–1302, (2010), doi: 10.1086/657021.
- [29] K. Mukai, V. Rana, F. Bernardini, and D. de Martino, ‘Unambiguous Detection of Reflection in Magnetic Cataclysmic Variables: Joint NuSTAR – XMM-NEWTON Observations of Three Intermediate Polars’, ApJ. **807**, 2, p. L30, (2015), doi: 10.1088/2041-8205/807/2/L30.
- [30] V. Suleimanov, V. Doroshenko, L. Ducci, G. V. Zhukov, and K. Werner, *GK Persei and EX Hydrae: Intermediate polars with small magnetospheres*, A&A, **591**, p. A35, (2016), doi: 10.1051/0004-6361/201628301.
- [31] R. A. García and J. Ballot, *Asteroseismology of solar-type stars*, Living Rev. Sol. Phys. **16**, 1, p. 4, (2019), doi: 10.1007/s41116-019-0020-1.
- [32] C. Aerts, *Probing the interior physics of stars through asteroseismology*, Rev. Mod. Phys. **93**, 1, p. 015001, (2021), doi: 10.1103/RevModPhys.93.015001.
- [33] R. A. García and J. Ballot, *Asteroseismology of solar-type stars*, Living Rev. Sol. Phys. **16**, 1, p. 10, (2019), doi: 10.1007/s41116-019-0020-1.